

Adaptive Range-Based Collision Avoidance MAC Protocol in Wireless Full-duplex Ad Hoc Networks

Yu Song^{1,2}, Wangdong Qi^{3*} and Wenchi Cheng⁴

¹ Institute of Command and Control Engineering, Army Engineering University, Nanjing, PR China, 210007

² Information and Communications College, National University of Defense Technology, Xi'an, PR China, 710106
[e-mail: ys_yusong@163.com]

³ National Mobile Communications Research Laboratory, Southeast University, Nanjing, PR China, 210096
[e-mail: wangdongqi@gmail.com]

⁴ State key Laboratory Services Networks, Xidian University, Xi'an, PR China, 710071
[e-mail: wccheng@xidian.edu]

*Corresponding author: Wangdong Qi

*Received Septebmer 13, 2017; revised February 16, 2018; revised November 1, 2018; accepted January 11, 2019;
published June 30, 2019*

Abstract

Full-duplex (FD) technologies enable wireless nodes to simultaneously transmit and receive signal using the same frequency-band. The FD modes could improve their physical layer throughputs. However, in the wireless ad hoc networks, the FD communications also produce new interference risks. On the one hand, the interference ranges (IRs) of the nodes are enlarged when they work in the FD mode. On the other hand, for each FD pair, the FD communication may cause the potential hidden terminal problems to appear around the both sides. In this paper, to avoid the interference risks, we first model the IR of each node when it works in the FD mode, and then analyze the conditions to be satisfied among the transmission ranges (TRs), carrier-sensing ranges (CSRs), and IRs of the FD pair. Furthermore, in the media access control (MAC) layer, we propose a specific method and protocol for collision avoidance. Based on the modified Omnet++ simulator, we conduct the simulations to validate and evaluate the proposed FD MAC protocol, showing that it can reduce the collisions effectively. When the hidden terminal problem is serious, compared with the existing typical FD MAC protocol, our protocol can increase the system throughput by 80%~90%.

Keywords: Wireless ad hoc networks, full-duplex communication, MAC protocol, collision avoidance, hidden terminal problem

This research was supported by This paper is supported by the National Natural Science Foundation of China (No. 61401330), Natural Science Foundation of Shaanxi Province of China (No. 2016JQ6027).

<http://doi.org/10.3837/tiis.2019.06.013>

ISSN : 1976-7277

1. Introduction

Recently, with the progress in self-interference (SI) cancellation technologies, the desired reception signals of the wireless nodes are no longer overwhelmed by the interference signals produced by themselves [1]. Typically, SI cancellation is divided into three modules, namely antenna cancellation, analog cancellation, and digital cancellation. They in turn process the interferece signal, as shown in Fig. 1.

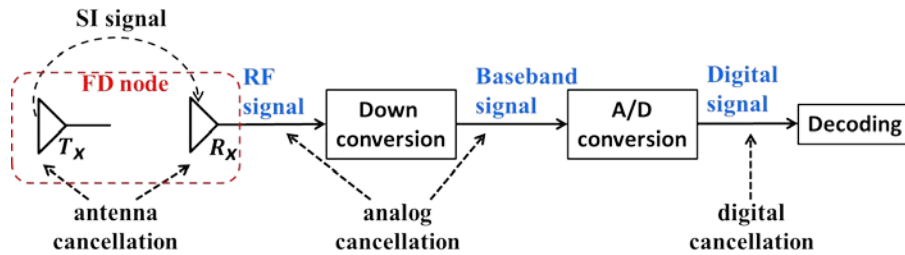


Fig. 1. Implementation principle of self-interference cancellation.

In Fig. 1, for the wireless full-duplex (FD) node, the T_x and R_x are the the transmitting antenna and the receiving antenna respectively. First, the antenna cancellation isolates the interference signal by optimizing the positions and directions of the two antennas. Second, we can delay the T_x signal and transmit it to the R_x through the wired link, which is used by the analog cancellation to offset the interference signal. Third, using digital signal process methods such as gradient descent, the digital cancellation further eliminates the remaining interference signal. Through these processes, the nodes can simultaneously transmit and receive using the same frequency-band. It is clear that the FD mode could improve the physical-layer throughputs of the nodes as compared with the half-duplex (HD) mode. Furthermore, it brings new opportunities for improving the spectral efficiencies [2] and throughputs of the networks, as shown in Fig. 2.



Fig. 2. The HD and FD communication modes.

However, in the wireless ad hoc networks, where the distance of each communication link may be different and each node operates in a distributed fashion, The FD communications also produce new interference risks [3]. On the one hand, the SI signals may reduce the signal-to-interference-noise-ratios (SINRs) of the nodes when they work in the FD mode, so that they are more likely to be interfered by other transmitted signals during their receptions. On the other hand, unlike the HD communications, each sender also receives the signal during its transmission. The potential hidden terminal problems would appear around the both sides of each FD pair. Thus, for the network-layer to fully benefit from the FD communications and to avoid the interference risks produced by them, designing a new mechanism in the media access control (MAC) layer is necessary [4].

The distributed coordination function (DCF) protocol is widely used in the MAC layers of the wireless HD ad hoc networks (“HD networks” for short). Each node uses the carrier-sensing multiple access (CSMA) mechanism to contend for the channel. Before a frame is

sent, if its size is larger than a given threshold, then the sender can first set up the Request-to-Send/Clear-to-Send (RTS/CTS) handshake with the receiver [5]. When the node in the interference range (IR) of the receiver can receive the CTS frame correctly or can sense the transmitted signal strength of the sender during its reception, we can avoid the hidden terminal problem. Under the two conditions, literatures [6] and [7] modeled the interference models for the HD nodes and proposed the specific methods for collision avoidance respectively.

Unfortunately, these models and methods cannot be applied to the wireless FD ad hoc networks ("FD networks" for short) directly. First, during the reception of a receiver, although its transmitted signal can enlarge the original carrier-sensing range (CSR), which is formed by the transmitted signal of the other side only, its IR is also enlarged by the SI signal. For each FD pair, the FD MAC mechanism first needs to reasonably model the IRs of the two sides and the CSR formed by the two transmitted signals, and then determines whether the FD mode is feasible. Second, each FD pair does not necessarily have the same size of the data frame. After the node with the smaller size sends the frame, it will receive the frame from the other side in the HD mode. However, the enlarged CSR has expired. The FD MAC mechanism needs to identify the size difference and avoid the interference risk of the remaining reception.

In this paper, we propose a MAC protocol for collision avoidance in FD networks. Under the wireless transmission model and the modeled FD interference model, we solve the TRs, CSRs and IRs of the nodes. To avoid the interference risks, we analyze the conditions to be satisfied among these ranges. We require the FD pair to get the values of the ranges by using the interaction of the designed control frames. If the FD mode cannot avoid the hidden terminal problems around the both sides, we require them to work in the HD mode. Furthermore, when the node with the smaller size of the data frame completes its transmission, to avoid the interference risk of the remaining reception, we determine whether it should take a further action and develop the specific mechanism. We conduct the simulations based on the modified Omnet++ simulator [8] to validate and evaluate the protocol. Simulation results show that it can reduce the collisions effectively. When the hidden terminal problem is serious, compared with the existing typical FD MAC protocol, our protocol can increase the system throughput by 80%~90%. In detail, we analyze the working process of the two protocols and the DCF protocol used in HD networks.

The rest of this paper is organized as follows. Section 2 introduces the related works for the FD MAC protocols in recent years. Section 3 presents the system model, including the FD interference model. Section 4 proposes our method for collision avoidance in FD networks. Section 5 describes the specific protocol. Section 6 simulates and analyzes the protocol performance. Section 7 concludes the paper.

2. Related Work

For backward compatibility, current research on the FD MAC protocol attempts to improve or extend the HD DCF protocol. Literature [9] proposed a simple CSMA-based FD MAC protocol to avoid hidden terminal problems, the receiver is required to send the supplementary signal while receiving from the sender. FD-MMAC in [10] extended the "busy tone" method in [9] to the multi-channel. Using the FD capabilities of the nodes, the protocol can adjust load strength among multiple channels. However, these works did not model the IR of the FD nodes properly. Literatures [11] and [12] extended the semantics of RTS/CTS control frames of the HD DCF protocol. Using their interactions, they managed to effectively coordinate the FD communications of the nodes and were able to avoid hidden terminal problems. However, none of them considered the wireless transmission model and the SI signals of the FD nodes.

Under realistic SI and network models, the proposed protocol in [13] can optimize the system throughput in a WLAN in which FD and HD nodes coexist. For the WLAN with an FD AP and several HD stations, literature [14] explored capture effect to provide the FD opportunities for the AP. In [15], a power control FD MAC protocol was proposed to maximize the system throughput by optimizing the transmit power of the uplink HD user and FD access nodes, as well as the downlink node selection. Although the transmit power, SINR, and other physical parameters were considered, these protocols were applied only to WLANs. There were no interference nodes outside the TRs of both the sender and receiver. Hidden terminal problems were not highlighted in such type of networks. For the wireless ad hoc networks, literature [3] deduced the upper bound of network capacity caused by FD communications. However, the interference model the authors used was the idealistic protocol model, where CSR was considered to be IR and we had a definite ratio between the TR and IR of each node. In addition, this work did not propose any feasible protocol implementation. To reduce the interference risk, in [16], each node of the FD pair was required to transmit the data frames using the maximum transmit power periodically, which formed the maximum CSR. But when the IR of the node was large, even the maximum CSR was not able to cover it. Literature [17] solved this problem, it required the two nodes to select the communication mode first. If the FD mode is not feasible, they should communicate in the HD mode. However, the two works also failed to give the proper definition of the IR of the FD nodes. In addition, they both assumed that the FD pairs have the same data frame size, which limits their applicable scenes.

3. System Model

We assume that there are several adjacent FD node pairs in wireless ad hoc networks and that these pairs all work in the bidirectional mode. We take nodes A and B as example and assume that A initializes the HD or FD communication. The transmit power of them are denoted by P_{t_A} and P_{t_B} . We have $P_{t_A}=P_{t_B}=P_t$. We denote by $\text{DataA} \rightarrow \text{B}$ and $T_{\text{DataA} \rightarrow \text{B}}$ the data frame sent from A to B and its transmission time, respectively. We denote by $L_{\text{DataA} \rightarrow \text{B}}$ the size of the $\text{DataA} \rightarrow \text{B}$ frame. If B receives the $\text{DataA} \rightarrow \text{B}$ frame correctly, it will reply the acknowledgement frame. We denote by $\text{AckB} \rightarrow \text{A}$ and T_{Ack} the frame and its transmission time. The signal power received by B from A and the SINR are denoted by $P_{r_{A \rightarrow B}}$ and $\text{SINR}_{A \rightarrow B}$, respectively. Similarly, we have the denotations $\text{DataB} \rightarrow \text{A}$, $\text{AckA} \rightarrow \text{B}$, $T_{\text{DataB} \rightarrow \text{A}}$, $L_{\text{DataB} \rightarrow \text{A}}$, $P_{r_{B \rightarrow A}}$, and $\text{SINR}_{B \rightarrow A}$. We denote by T_{diff} the difference between $T_{\text{DataA} \rightarrow \text{B}}$ and $T_{\text{DataB} \rightarrow \text{A}}$.

3.1 Wireless Transmission Model

The signal propagation attenuation between A and B obeys the two-way ground-reflection model. The $P_{r_{A \rightarrow B}}$ is defined as follows:

$$P_{r_{A \rightarrow B}} = c \frac{P_{t_A}}{D_{AB}^4}, \quad (1)$$

where D_{AB} denotes the distance between A and B, while c is a constant that is determined by the heights and gains of the antennae of A and B. We can obtain the $\text{SINR}_{A \rightarrow B}$ as follows:

$$\text{SINR}_{A \rightarrow B} = \frac{P_{r_{A \rightarrow B}}}{P_{n_B}} > \text{SINR}_{\text{thold}}, \quad (2)$$

where P_{n_B} denotes the total interference power received by B, and is obtained as follows:

$$P_{n_B} = \sum_{L \neq A} G_{LB} P_{t_L} + S I_B P_{t_B} + P_n, \quad (3)$$

where $G_{LB}Pt_L$, SI_BPt_B , and P_n denote the interference power for B from the other nodes, the SI power of B (SI_B is the SI coefficient of B), and the background noise power, respectively. Similarly, we have the expressions $Pr_{B \rightarrow A}$, $SINR_{B \rightarrow A}$, and $Pn_A(SI_A)$. Moreover, Pr_{thold} and $SINR_{thold}$ represent the minimum power and SINR bounds for the correct reception of desired signals. Ps_{thold} represents the minimum power bound for the nodes to be able to sense a signal. We assume $Pt_A=281.2$ mw, as D_{AB} increases, the values of $Pr_{A \rightarrow B}$ are shown in Fig. 3.

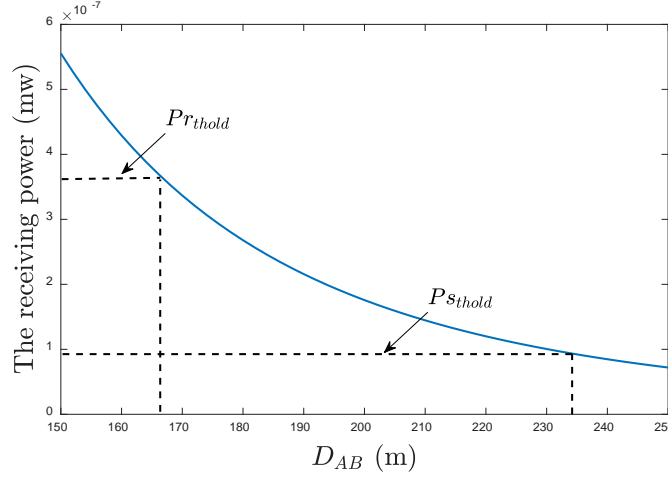


Fig. 3. The values of $Pr_{A \rightarrow B}$ versus the different values of D_{AB} .

Here, we set Pr_{thold} and Ps_{thold} to 3.652×10^{-7} mw and 0.95×10^{-7} mw respectively.

TR_A and CSR_A denote the TR and CSR of A, respectively. The frames sent by A can be successfully received by the nodes within TR_A , but can only be sensed by the nodes within CSR_A . In other words, the receiving signals of the nodes within TR_A are required to satisfy both Pr_{thold} and $SINR_{thold}$ constraints, while the receiving signals of the nodes within CSR_A are only required to satisfy Ps_{thold} constraint. Note that the background noise power is low, when a node receives the signal in the HD mode and there are no other nodes transmitting signals at the same time, $SINR_{thold}$ constraint can be easily satisfied, TR_A is determined by Pr_{thold} constraint. At this time, CSR_A is δ ($\delta > 1$) times TR_A , where δ is determined by the physical properties of nodes. In Fig. 3, $TR_A=167$ m, $CSR_A=233$ m. During the reception of a node, if it transmits the signal or other nodes transmit the signals simultaneously, the interference power will reduce its receiving SINR. The desired signal power may not satisfy $SINR_{thold}$ constraint. The above relationship between TR_A and CSR_A is not necessarily true. Similarly, we have the denotations TR_B and CSR_B . Moreover, we denote by CSR_{AB} the CSR of A and B transmitting signals simultaneously.

IR_B denotes the IR of B, the transmitted signals within IR_B can interfere with the reception of the DataA \rightarrow B frame. Similarly, we have the denotation IR_A .

3.2 FD Interference Model

Let Prn_B be the remaining noise power level that B can tolerate. In order to satisfy the $SINR_{thold}$ constraint, Prn_B is required to satisfy the following inequality:

$$Prn_B \leq \frac{Pr_{A \rightarrow B}}{SINR_{thold}} - SI_BPt_B - P_n. \quad (4)$$

Let B' be the closest neighbor not to interfere with the reception at B. We require that:

$$c' \frac{Pt_{B'}}{D_{B'B}^4} \leq Prn_B, \quad (5)$$

where the definitions of c' and $D_{B'B}$ are consistent with those of c and D_{AB} respectively. By Eq. (1) and Eq. (4), Eq. (5) can be rewritten as follows:

$$c' \frac{Pt_{B'}}{D_{B'B}^4} \leq \frac{cPt_A}{D_{AB}^4 SINR_{thold}} - SI_B Pt_B - P_n \quad (6)$$

We transform the form of Eq. (6). The constraint that $D_{B'B}$ needs to satisfy is as follows:

$$D_{B'B} \geq \left(\frac{c'}{\frac{c}{D_{AB}^4 SINR_{thold}} - SI_B - \frac{P_n}{Pt}} \right)^{\frac{1}{4}} \quad (7)$$

Thus, $\left(\frac{c'}{\frac{c}{D_{AB}^4 SINR_{thold}} - SI_B - \frac{P_n}{Pt}} \right)^{\frac{1}{4}}$ is the IR when B works in the FD mode, denoted by

$IR_B(\text{FD})$. We remove the SI_B item of Eq. (7), $\left(\frac{c'}{\frac{c}{D_{AB}^4 SINR_{thold}} - \frac{P_n}{Pt}} \right)^{\frac{1}{4}}$ is the IR when B works

in the HD mode [6], denoted by $IR_B(\text{HD})$. For simplicity, we let $P_n/Pt=0$, because $P_n \ll Pt$. In addition, both the values of c and c' are set to 1. Hence, $IR_B(\text{FD})$ is determined by both D_{AB} and SI_B , whereas $IR_B(\text{HD})$ is determined by D_{AB} only. In a similar manner, we have the expressions $IR_A(\text{FD})$ and $IR_A(\text{HD})$.

4. The Proposed Method for Collision Avoidance in FD Networks

We first summarize the methods for collision avoidance in HD networks. Then we discuss the interference risks in FD networks and propose a specific method to avoid them. In this section, when $T_{diff} \neq 0$, for simplicity, we always assume that $T_{DataA \rightarrow B} > T_{DataB \rightarrow A}$.

4.1 Methods Summary for Collision Avoidance in HD Networks

In HD networks, according to the HD DCF protocol, there are mainly two methods for collision avoidance.

MethodA: After B successfully receives the RTS frame from A, it replies the CTS frame, the TR of which is used to cover $IR_B(\text{HD})$ [5][6], as shown in Fig. 4(a). The nodes within $IR_B(\text{HD})$ reserve the virtual carrier-sensing time according to the value of the “Duration” (“D” for short) field of the CTS frame and do not send signals during the reception of the DataA→B frame.

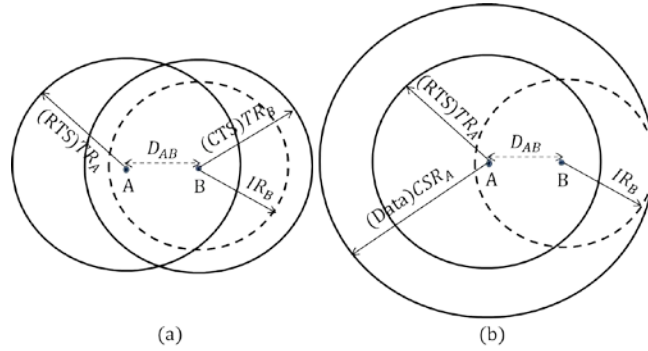


Fig. 4. The schematic diagram of the two methods for collision avoidance in HD networks.

MethodB: Let the CSR_A cover IR_B (HD)[7], as shown in **Fig. 4(b)**. During the transmission of the DataA→B frame, the nodes within IR_B (HD) can always sense the channel busy. After the transmitted signal disappears, they will delay the EIFS time ($SIFS+T_{Ack}$) before contending for the channel.

It is clear that $TR_B > IR_B$ (HD) and $CSR_A > D_{AB} + IR_B$ (HD) are the two conditions for collision avoidance of the two methods respectively.

4.2 Interference Risks Produced by FD Communications

In FD networks, B transmits the signal while receiving the signal from A simultaneously. CSR_{AB} enlarges CSR_A . From the perspective of IR_B (FD) coverage, the effectiveness of using CSR_{AB} is better than that of using TR_B or CSR_A . However, IR_B (FD) increases as SI_B increases. Once the value of SI_B is large, IR_B (FD) cannot be covered by CSR_{AB} as well. The interference risk of the data frame reception still exists.

Moreover, the size difference between the DataA→B and DataB→A frames produces another interference risk. After B sends the DataB→A frame, CSR_{AB} will reduce to CSR_A . The nodes first located in CSR_{AB} but not within CSR_A afterward only reserve the EIFS time, then contend for the channel. When $T_{diff} > EIFS$, these transmitted signals may interfere with the remaining reception of the DataA→B frame. However, when $T_{diff} \leq EIFS$, although CSR_{AB} reduces after B send the DataB→A frame, B will complete the reception within the EIFS time, during which the nodes located in the original CSR_{AB} will not produce any interference signals.

4.3 The Proposed Method

According to the discussion above, based on the difference between the T_{diff} and the EIFS time, we discuss the method for collision avoidance in FD networks in the following two cases.

- 1). Collision avoidance method when $T_{diff} = 0$ or $\leq EIFS$.

When A communicates with B in the FD mode, during the simultaneous transmissions of the DataA→B and DataB→A frames, the nodes within IR_A (FD) and IR_B (FD) are not able to send signals. We use CSR_{AB} to cover both IR_A (FD) and IR_B (FD). We model CSR_{AB} and IR_B in a two-dimensional polar coordinate system with r and θ to analyze the effective condition of the method, as shown in **Fig. 5**. IR_A can be modeled in a similar manner.

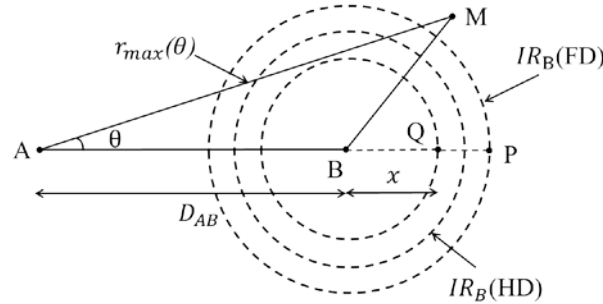


Fig. 5. The schematic diagram of CSR_{AB} and IR_B in a two-dimensional polar coordinate system.

Let A be the origin (0,0) of the coordinate system. The direction of \overrightarrow{AB} is taken as the direction of $\theta=0$. The position P is in this direction. We have $D_{BP}=IR_B(FD)$. In the direction of θ , we assume that M is the farthest position where the signals transmitted from A and B can be sensed. D_{AM} in our coordinate system is also denoted by $r_{max}(\theta)$. On the one hand, as θ varies in the range of $[0, 2\pi]$, CSR_{AB} is the envelop formed by $r_{max}(\theta)$. On the other hand, when B works in the FD mode, its IR is a circle centered at the position of B with the radius of $IR_B(FD)$. Note that it is difficult to obtain the analytic expression of $r_{max}(\theta)$, so we are not able to discuss whether $IR_B(FD)$ can be covered by CSR_{AB} directly. Note that at the boundary of $IR_B(FD)$, B produces the same receiving signal strength, but only at the position of P, does A produce the minimum receiving signal strength. In addition, according to Eq. (7), $IR_B(FD)$ is determined by both D_{AB} and SI_B . Thus, given D_{AB} and SI_B , if we have the following condition:

$$\frac{1}{\left(D_{AB} + \frac{1}{\left(\frac{1}{D_{AB}^4 SINR_{thold}} - SI_B \right)^{\frac{1}{4}}} \right)^4} + \frac{1}{\left(\frac{1}{\left(\frac{1}{D_{AB}^4 SINR_{thold}} - SI_B \right)^{\frac{1}{4}}} \right)^4} \geq \frac{Ps_{thold}}{Pt} \quad (8)$$

CSR_{AB} can then cover the whole of $IR_B(FD)$. This condition is both the sufficient and necessary to cover $IR_B(FD)$. Similarly, to cover $IR_A(FD)$, we have the following sufficient and necessary condition:

$$\frac{1}{\left(\frac{1}{\left(\frac{1}{D_{AB}^4 SINR_{thold}} - SI_A \right)^{\frac{1}{4}}} \right)^4} + \frac{1}{\left(D_{AB} + \frac{1}{\left(\frac{1}{D_{AB}^4 SINR_{thold}} - SI_A \right)^{\frac{1}{4}}} \right)^4} \geq \frac{Ps_{thold}}{Pt} \quad (9)$$

If the values of SI_A and SI_B remain unchanged, then for D_{AB} , both the functions in Eqs. (8) and (9) are monotonic. Thus, we can easily solve the two values of D_{AB} respectively. The maximum value of D_{AB} which satisfies the both conditions is the cut-off point to determine whether A can communicate with B in the FD mode.

2). Collision avoidance method when $T_{diff} > \text{EIFS}$.

After B sends the DataB→A frame, the transmitted signal from B disappears. B receives the remainder of the DataA→B frame in the HD mode. We first observe whether the effective condition of the **MethodB** holds, if so, the transmitted signal of the remaining data frame itself can avoid the nodes within $IR_B(\text{HD})$ transmitting signals. Otherwise, we have to develop an extra method.

Intuitively, if the effective condition of the **MethodA** holds, that is $TR_B > IR_B(\text{HD})$, there are two methods available.

First, before the two nodes send the data frames, during the interaction of the control frames, B uses the “D” field of the control frame to set virtual carrier-sensing time for the nodes within $IR_B(\text{HD})$. The value of the “D” field is determined by the $T_{DataA \rightarrow B}$ (the larger one). Typically, [11], [12] and [16] adopted a three-handshake mechanism. However, in a network with dense nodes, although some nodes are within TR_B , their receptions of the control frame are more likely to be interfered by other transmitted signals, so that they cannot obtain the “D” field of that frame. At this time, using the “D” field to set the virtual carrier-sensing time for the nodes within $IR_B(\text{HD})$ is ineffective.

Second, after B sends the DataB→A frame, B then sends a supplementary (“ADD” for short) frame. The value of the “D” field is determined by $T_{DataA \rightarrow B} - T_{DataB \rightarrow A}$. Since B just sends over, the nodes within the original CSR_{AB} will not transmit the signals in the future EIFS time ($T_{ADD} < \text{EIFS}$). Meanwhile, we have $CSR_{AB} > CSR_B > TR_B$. The nodes within the TR_B are less likely to be interfered during the reception of the ADD frame. However, this method is ineffective under the actual signal attenuation and interference models. This is because that during the transmission of the ADD frame, B still communicates with A in the FD mode. The nodes within TR_B will receive the signal transmitted by A, which is considered as the interference signal. When the SINR cannot satisfy SINR_{thold} constraint, the nodes cannot obtain the value of the “D” field of the ADD frame. In other words, compared with the TR of B sending a frame alone, the TR of the ADD frame will reduce. In the most optimistic case, we discuss the relationship of the sizes of the reduced TR and $IR_B(\text{HD})$. In Fig. 5, we model a circle centered at the position of B with the radius of x , denoted by $O(B, x)$. Q is a position in the direction of $\theta=0$. We have $D_{BQ}=x$. Similar to the above discussion, at the boundary of $O(B, x)$, B produces the same receiving signal strength, which can be calculated by Pt_B/x^4 ; but at the position of Q, A produces the minimum receiving signal strength, which can be calculated by $Pt_A/(D_{AB}+x)^4$. Note that the signal from A is the interference signal for the nodes around B. Therefore, it is at the position of Q that the ADD frame sent by B has the largest SINR. Given D_{AB} , the largest value of x can be derived from the following inequality:

$$\frac{(D_{AB} + x)^4}{x^4} \geq \text{SINR}_{thold} \quad (10)$$

For one thing, the largest x is the largest TR of B sending the supplementary frame. We denote it by TR_B' . For another, according to [5], we have $IR_B(\text{HD})=1.78D_{AB}$. We substitute $x=1.78D_{AB}$ into Eq. (10), the inequality does not hold, which means that $TR_B' < IR_B(\text{HD})$. In other words, at the boundary of $IR_B(\text{HD})$, the nodes cannot properly receive the ADD frame even at the position where the interference signal strength is the smallest. Thus, they may contend for the channel during the remaining reception of the DataA→B frame.

Therefore, after B sends the DataB→A frame, if $CSR_A > D_{AB} + IR_B(\text{HD})$ cannot be satisfied, we require B to transmit the supplementary signal, which are used to maintain the effectiveness of CSR_{AB} during the remaining reception of the data frame. In practice, the

method can be implemented by sending several ADD frames. Note that after each ADD frame is sent, the nodes within CSR_{AB} will reserve the EIFS time, so we set the transmission interval of the ADD frames to the EIFS time for energy efficiency. At the same time, we require that after B sends the last ADD frame, it can receive the DataA→B frame within the EIFS time. We denote by T_{ADD} and N_{ADD} the transmission time and number of the ADD frames, respectively. N_{ADD} can be obtained as follows:

$$N_{ADD} = \left\lceil \frac{T_{DataA \rightarrow B} - T_{DataB \rightarrow A}}{T_{ADD} + EIFS} \right\rceil, \quad (11)$$

where the “ $\lceil \cdot \rceil$ ” symbol represents rounding up. The transmission interval between the last ADD frame and its previous one is determined by whether the following inequality can be satisfied:

$$(T_{DataA \rightarrow B} - T_{DataB \rightarrow A}) \bmod (T_{ADD} + EIFS) > T_{ADD}, \quad (12)$$

where the “mod” symbol represents modulus calculation. If it holds, the interval is the EIFS time, as shown in Fig. 6(a); otherwise, there is no interval time, as shown in Fig. 6(b).

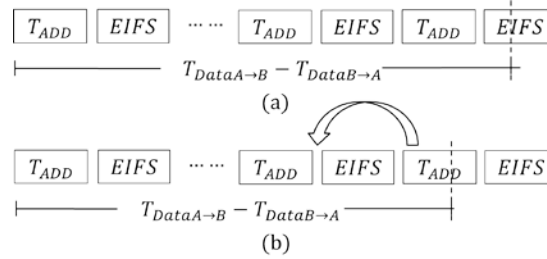


Fig. 6. The transmission interval between the last ADD frame and its previous one.

5. The Proposed FD MAC Protocol in FD Networks

In order to apply the method above to the network, we propose an FD MAC protocol for collision avoidance. First, we introduce the structures and semantics of the control frames used in our protocol. Subsequently, we describe the working process of the protocol.

5.1 Structures and Semantics of Control Frames

Our protocol uses three types of control frames: RTS-SI, CTS-M and ADD, the structures of them are shown in Fig. 7.

RTS-SI	Frame Control	Duration ID	Receiver Address	Transmitter Address	SI Coefficient	FCS
Bytes	2	2	6	6	2	4
CTS-M	Frame Control	Duration ID	Receiver Address	Communication mode	FCS	
Bytes	2	2	6	2	4	
ADD	Frame Control	Duration ID	Receiver Address	FCS		
Bytes	2	2	6	4		

Fig. 7. The structures of RTS-SI, CTS-M and ADD frames.

Compared with the RTS and CTS frames used in the HD DCF protocol, the fields “SI Coefficient” (“SI” for short) and “Communication Mode” (“M” for short) are added in the RTS-SI and CTS-M frames, respectively. The former is used to store the values of the SI coefficients of the nodes while the latter is used to specify the communication mode for each FD pair (“2” for FD, “1” for HD).

5.2 Protocol Rules

For an FD pair, the two senders can contend for the channel. We need to clarify the following two issues:

First, to obtain the value of the SI coefficient accurately, we require that each node should transmit a dedicated signal for the coefficient estimation before it starting a new transmission, which costs T_{SI} time. When a node senses other signals during the transmission of the estimation signal, it deems that the value of the SI coefficient is invalid and re-contentends for the channel. At a time slot, both the back-off counts of the two senders may decrease to 0, and they send the frames for each other. Although they can receive the frames from the other side and take the following actions, since we require them to transmit the SI estimation signal first, in such case, they have to give up the current transmission and jump to the back-off states. Besides, excluding the data frames, other frames (control frames and Ack frame) are required to send or receive in the HD mode. In particular, we provide that one side of the FD pair with smaller size of the data frame first send the Ack frame to the other side.

Second, according to the DCF protocol, we can model the states and their transitions of each sender to a Markov chain [18], as shown in the non-red line part of Fig. 8.

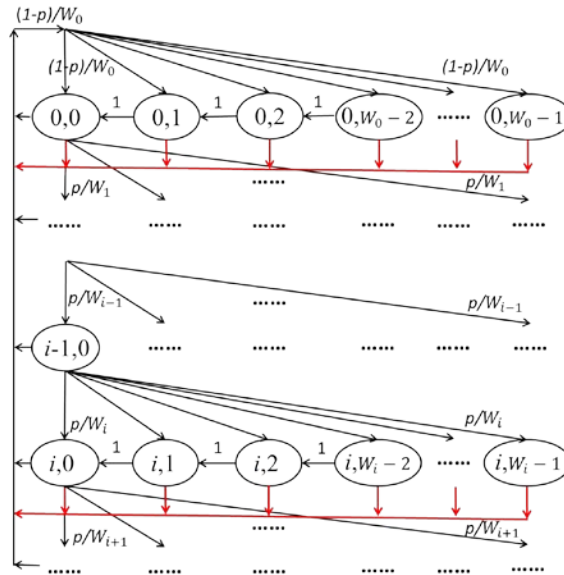


Fig. 8. The states and their transitions of each sender.

In Fig. 8, i and p represent the back-off stage and collision probability respectively. For the FD communication, the following situation may occur: A sends the frame to B, but B does not reply on time (It may sense the channel busy or has been set the virtual carrier-sensing time). If A waits for a timeout, then it will increase the back-off stage and re-select the back-off count in the new contention window. Note that when B obtains the opportunity for accessing the channel, it will set up an FD communication with A. That is, A may complete the transmission

of the DataA→B frame passively. At this time, no matter which back-off stage A is in, we require it to jump to the back-off stage 0. In such case, the transitions of the states are shown in the red line part of Fig. 8.

5.3 Protocol Description

Before A sends the DataA→B frame, it first senses the channel. When it is idle, A transmits SI_A estimation signal. During its transmission, once A senses other signals, it will jump to the back-off states. Otherwise, A considers that the value of SI_A is valid and then fills it to the “SI” field of the RTS-SI frame. At the same time, A sets the value of the “D” field of the frame according to $T_{DataA→B}$. Then, A sends the RTS-SI frame to B.

After B senses the estimation signal, it will receive the RTS-SI frame sent by A. If the value of $SINR_{A→B}$ varies more than a certain range, the received RTS-SI frame is considered to be inaccurate and B will not reply the CTS-M frame to A. Otherwise, B gets the values of SI_A and $T_{DataA→B}$ from the RTS-SI frame and calculates the value of D_{AB} according to the strength of the receiving signal. Then, B transmits SI_B estimation signal. Note that if B senses other signals during the transmission of SI_B estimation signal, B is unable to communicate with A in the FD mode because it does not obtain the accurate SI coefficient. B sets the value of the “M” field of the CTS-M frame to 1 (for HD) directly. Otherwise, based on the values of $T_{DataB→A}$, $T_{DataA→B}$, D_{AB} , δ , SI_B and SI_A , B specifies the communication mode and uses the specific method for collision avoidance.

Specifically, if CSR_{AB} cannot cover $IR_A(FD)$ and $IR_B(FD)$ simultaneously, the value of the “M” field of the CTS-M frame is set to 1 (for HD). Furthermore, if $CSR_A > D_{AB} + IR_B(HD)$, B sets the value of the “D” field of the CTS-M frame to 0. Otherwise, the value is determined by the value of $T_{DataA→B}$ to reserve the channel for the reception of the DataA→B frame. If CSR_{AB} can cover $IR_A(FD)$ and $IR_B(FD)$ simultaneously, B sets the value of the “M” field of the CTS-M frame to 2 (for FD). If $T_{DataB→A} > T_{DataA→B}$, the value of “D” field of the CTS-M frame is determined by $T_{DataB→A}$, which is used to deliver the value of $T_{DataB→A}$ to A. After sending the CTS-M and the DataB→A frames, B waits T_{Ack} time, then sends the AckB→A frame if it has received the DataA→B frame correctly. Here the T_{Ack} time is the reserving time for B to receive the AckA→B frame. Otherwise, that is $T_{DataA→B} > T_{DataB→A}$, the value of the “D” field of the CTS-M frame is set to 0, which means that B does not need to inform A of the value of $T_{DataB→A}$. Furthermore, if $T_{DataA→B} - T_{DataB→A} \leq EIFS$, or $T_{DataA→B} - T_{DataB→A} > EIFS$ and $CSR_A > D_{AB} + IR_B(HD)$, B only needs to reply the AckB→A frame after receiving the DataA→B frame correctly. If we only have $T_{DataA→B} - T_{DataB→A} > EIFS$, but $CSR_A > D_{AB} + IR_B(HD)$ cannot be satisfied, after B sends the DataB→A frame, it will send several ADD frames, the sending number of which is determined by Eq. (11) and their sending time are shown in Fig. 6.

After A receives the CTS-M frame, it gets the values of the “M” and “D” fields and sets up the FD or HD communication with B. Specifically, if the value of the “M” field is 1, A sets up the HD communication with B. After A sends the DataA→B frame, it just waits the AckB→A frame back. If the value of the “M” field is 2 and the value of the “D” field does not equal to 0, which means that $T_{DataB→A} > T_{DataA→B}$. After A sends the DataA→B frame, similar to the above discussion, if we only have $T_{DataB→A} - T_{DataA→B} > EIFS$, but $CSR_B > D_{AB} + IR_A(HD)$ cannot be satisfied, A will send several ADD frames. Otherwise, A just needs to send the AckA→B frame after correctly receiving the DataB→A frame. If the value of the “M” field is 2 but the value of the “D” field equals to 0, after A sends the DataA→B frame, it waits T_{Ack} time, and then sends the AckA→B frame if it has received the DataB→A frame correctly.

5.4 Key Points of Our Protocol Operation

For the proposed protocol, we describe the transmission and reception behaviors of the antenna in the physical-layer. We also describe the states and their transitions of each sender in the MAC-layer when it works in the FD mode.

The processing flow when the antenna starts to sense a frame is shown in **Fig. 9**.

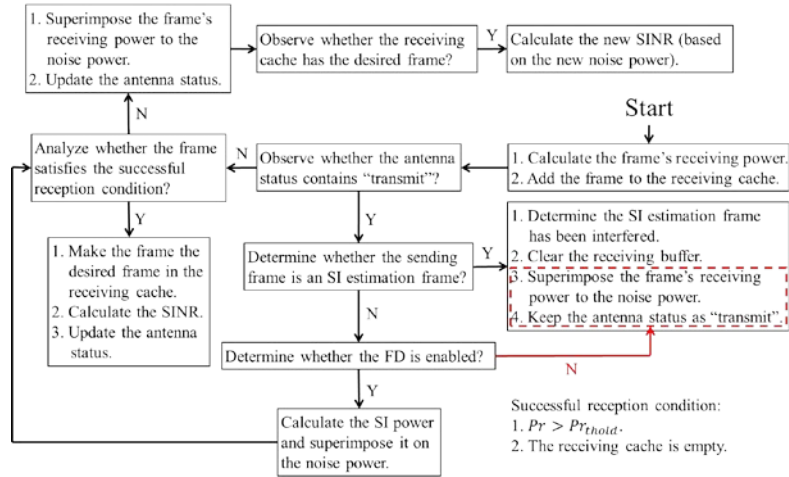


Fig. 9. The processing flow when the antenna starts to sense a frame.

We conduct a receiving cache to store all the received frame. We also mark the desired frame. Combined with the working mode of the node, we update the SINR of the desired frame and the state of the antenna in real time.

The processing flow when the antenna completes sensing a frame is shown in **Fig. 10**.

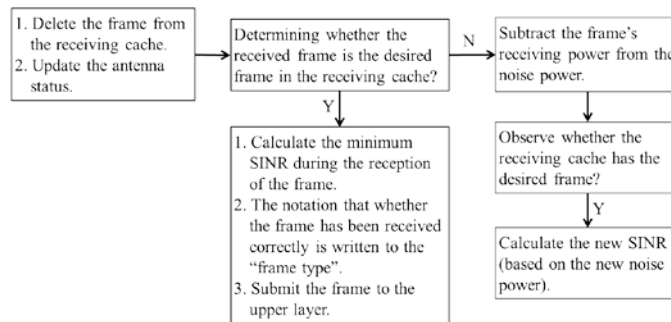


Fig. 10. The processing flow when the antenna completes sensing a frame.

When the antenna completes sensing a frame, it determines whether the frame is the desired frame. If so, it further determines whether the frame has been received correctly. Otherwise, it only updates the noise power.

The processing flow when the antenna starts to send a frame is shown in **Fig. 11**.

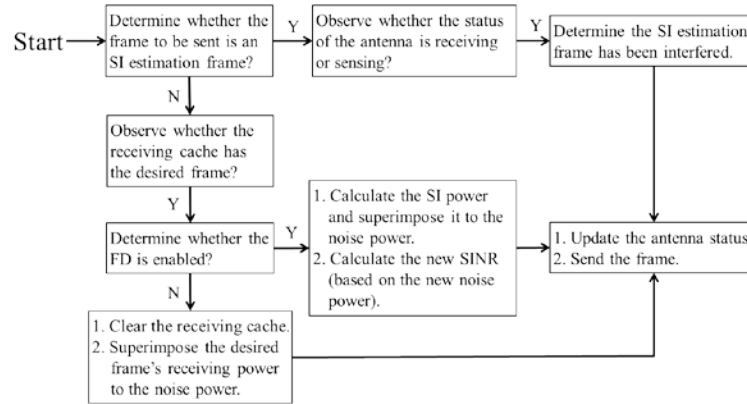


Fig. 11. The processing flow when the antenna starts to send a frame.

When the antenna starts to send a frame, if it is an SI estimation signal, it needs to determine whether the signal is interfered according to the antenna state. Otherwise, it needs to manage the receiving cache and update the noise power.

When the node works in the FD mode, the states and their transitions of the node in the MAC-layer are shown in Fig. 12.

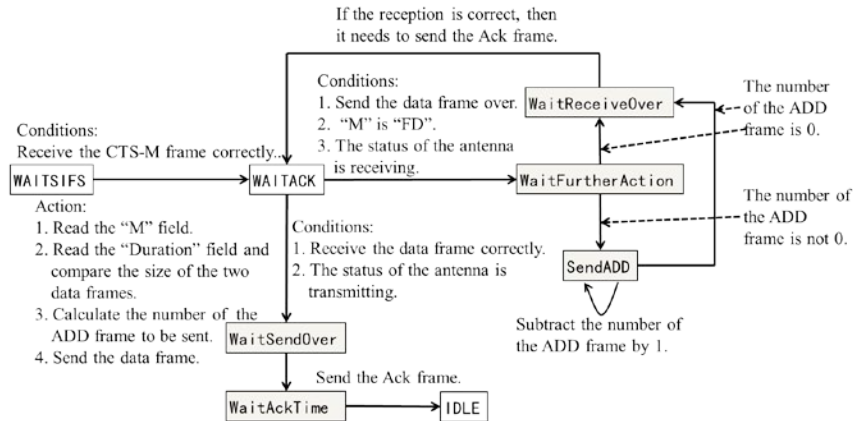


Fig. 12. The states and their transitions of the node in the MAC-layer when it works in the FD mode.

For the FD communication, note that the sizes of the two frames may be inconsistent and the transmissions of the two Ack frames have a priority. Hence, we define a number of new states (filled in grayscale). The state transitions not covered in Fig. 12 are consistent with those in the original DCF state machine.

5.5 Duration Time and Timeout Time of Frames

In detail, we set the duration time and timeout time of the control frames and data frames mentioned above.

The value of the "D" field of the RTS-SI frame is set to $4 \times \text{SIFS} + T_{SI} + T_{CTS-M} + T_{DataA \rightarrow B} + T_{Ack}$. In the following two cases, the CTS-M frames need to set the value of the "D" field. When A sends the DataA→B frame in the HD mode and $CSR_A > D_{AB} + IR_B(\text{HD})$ cannot be satisfied, the value of "D" field of the CTS-M frame is set to $2 \times \text{SIFS} + T_{DataA \rightarrow B}$. When B communicates with A in the FD mode and $T_{DataB \rightarrow A} > T_{DataA \rightarrow B}$, B needs to deliver the value of $T_{DataB \rightarrow A}$ to A, meanwhile, reserve the channel for the reception of the AckA→B frame. Therefore, the value

of the “D” field is set to $2 \times \text{SIFS} + T_{\text{DataB} \rightarrow \text{A}} + T_{\text{Ack}}$. Besides, the values of the “D” field of the CTS-M frame are all set to 0. If A or B needs to send ADD frames, the value of its “D” field is set to the EIFS time. Note that when A communicates with B in the FD mode, we do not use the duration times of the two data frames to reserve the channel. We set the values as they used in the HD DCF protocol.

After a node sends the RTS-SI frame, its timeout time is set to $2 \times \text{SIFS} + T_{\text{SI}} + T_{\text{CTS-M}}$. The CTS-M and ADD frames do not need reply. Hence, after a node sends them, we do not need to set the timeout time. When A communicates with B in the HD mode, its timeout time is set to $\text{SIFS} + T_{\text{Ack}}$. When A communicates with B in the FD mode, we assume that $T_{\text{DataA} \rightarrow \text{B}} > T_{\text{DataB} \rightarrow \text{A}}$, after A receives the DataB \rightarrow A frame, it can only reply the AckA \rightarrow B frame after it sends the DataA \rightarrow B frame. Furthermore, according to our protocol rule, the AckB \rightarrow A frame is sent before the AckA \rightarrow B frame. Therefore, after the two nodes send the DataA \rightarrow B frame and the DataB \rightarrow A frame respectively, we set the timeout time of them to $\text{SIFS} + T_{\text{Ack}}$ and $2 \times \text{SIFS} + T_{\text{DataA} \rightarrow \text{B}} - T_{\text{DataB} \rightarrow \text{A}} + 2 \times T_{\text{Ack}}$ respectively.

6. Protocol performance

In HD networks, the values of D_{AB} and δ determine the effectiveness of the existing two methods for collision avoidance. But in FD networks, the method for collision avoidance varies according to the size difference between T_{diff} and the EIFS time. At the same time, the values of D_{AB} , δ and $SI_B(SI_A)$ determine whether the relevant conditions are effective. We first conduct the numerical analysis for $IR_B(\text{FD})$, CSR_A , CSR_{AB} and the TR_B of the ADD frame. Then based on the modified Omnet++ simulator, we conduct a simulation using two FD pairs to validate and evaluate the proposed protocol.

6.1 Numerical Analysis for Ranges

We set δ to 1.4 and 1.5623, and set SI_B to 0, 0.5×10^{-9} and 1.5×10^{-9} . In addition, P_t , Pr_{thold} and $SINR_{\text{thold}}$ are set to 281.8mw, 3.652×10^{-7} mw, and 10, respectively. The numerical results are measured in terms of the distance away from B in the direction of $\theta=0$ of the modeled polar coordinate system in Fig. 5.

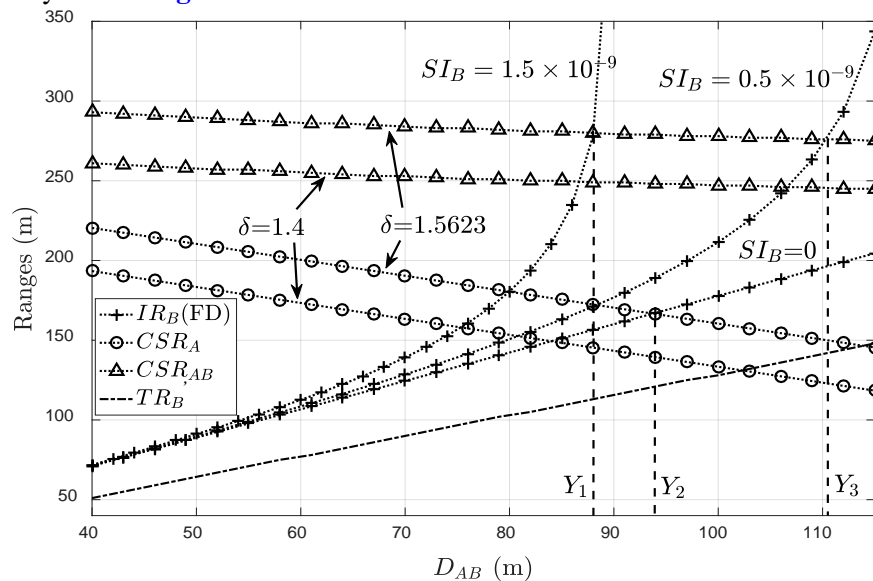


Fig. 13. The values of $IR_B(\text{FD})$, CSR_A , CSR_{AB} and the TR_B with the given δ and SI_B .

As shown in Fig. 13, if δ increases from 1.4 to 1.5623, using the same transmit power can produce a larger CSR , thus, both CSR_A and CSR_{AB} increase. We remain δ unchanged and discuss the changes of CSR_A and CSR_{AB} as D_{AB} increases. Note that the values of CSR_A and CSR_{AB} are measured relative to the position of B. Moreover, the former is determined by P_{t_A} alone, the latter is determined by both P_{t_A} and P_{t_B} . In particular, the part of CSR_{AB} which determined by P_{t_B} is independent of D_{AB} . Thus, as D_{AB} increases, both CSR_A and CSR_{AB} will reduce, but CSR_{AB} does not change much as compared with CSR_A . If D_{AB} remains unchanged as SI_B increases, $IR_B(\text{FD})$ will increase. When $SI_B=0$, the curve of $IR_B(\text{FD})$ is consistent with that of $IR_B(\text{HD})$. With regard to D_{AB} , Y_2 is the horizontal ordinate of the cross point of CSR_A ($\delta=1.5623$), TR_B and $IR_B(\text{HD})$. Y_2 is also the cut-off point to determine whether $TR_B > IR_B(\text{HD})$, which is the value of “0.56 TR_B ” in [5]. If $\delta=1.5623$, when $SI_B=0.5 \times 10^{-9}$ and 1.5×10^{-9} respectively, For D_{AB} , Y_1 and Y_3 are the two horizontal ordinates of the cross points of CSR_{AB} and $IR_B(\text{FD})$, which can be solved by Eqs. (8) and (9). Y_1 and Y_3 are also the two cut-off points to determine whether $CSR_{AB} > IR_B(\text{FD})$. Similarly, for different values of δ and SI_B , we can obtain the horizontal ordinates of the cross points of CSR_{AB} (or CSR_A) and $IR_B(\text{FD})$. All these horizontal ordinates are the cut-off points to determine whether CSR_{AB} (or CSR_A) can cover $IR_B(\text{FD})$. For brevity, we ignore their marks. As the curves of TR_B and $IR_B(\text{FD})$ ($SI_B=0$) shown in Fig. 13, for varied D_{AB} , the largest values of TR_B formed by B sending the ADD frame are always lower than those of $IR_B(\text{HD})$. This is consistent with the previous analysis.

6.2 Simulation Scenario and Parameter Settings

We conduct a simulation using two FD pairs: A and B, C and D, respectively, as shown in Fig. 14. Each node has a saturated queue of the data frames to send to the other side and contends for the channel independently.



Fig. 14. Simulation topology.

We assume that $L_{DataA \rightarrow B} = L_{DataD \rightarrow C}$, $L_{DataB \rightarrow A} = L_{DataC \rightarrow D}$, $SI_B = SI_C$, and $D_{AB} = D_{CD}$. We also assume that $L_{DataA \rightarrow B} / L_{DataD \rightarrow C} > L_{DataB \rightarrow A} / L_{DataC \rightarrow D}$ to set the interference risk produced by the size difference. On the one hand, after B/C sends the frame, according to whether CSR_A / CSR_D can cover $IR_B(\text{HD}) / IR_C(\text{HD})$, our protocol requires B/C to take different action. On the other hand, whether $C \in IR_B(\text{FD}) / B \in IR_C(\text{FD})$ determines if the interference risk of the remaining reception of the DataA \rightarrow B / DataD \rightarrow C frame exists. For comprehensively evaluating the protocol, in the simulation, we require that all the inclusion relations should appear. We set the varieties of D_{AB} / D_{CD} and D_{BC} to satisfy this requirement. The values of P_t , Pr_{thold} and $SINR_{thold}$ equal to those used in section 6.1. Other parameters are given in Table 1.

Table 1. Simulation parameters.

Parameter	Value
simulation time	100 s
D_{AB} / D_{CD}	80, 90 m
transmission rate	1 Mbps
SI_B / SI_C	0.5×10^{-9}
δ	1.4
$L_{DataA \rightarrow B} / L_{DataD \rightarrow C}$	1500 B
$L_{DataB \rightarrow A} / L_{DataC \rightarrow D}$	1000 B

According to the parameters given above, we can derive $TR_B/TR_C=167$, which does not change as D_{AB}/D_{CD} or D_{BC} changes. The values of $IR_B(\text{FD})$, $IR_B(\text{HD})$, CSR_A and CSR_{AB} are shown in Table 2.

Table 2. The values of $IR_B(\text{FD})$, $IR_B(\text{HD})$, CSR_A and CSR_{AB} with $\delta=1.4$ and varied D_{AB}/D_{CD} .

$D_{AB}/D_{CD}=80$ m		$D_{AB}/D_{CD}=90$ m	
Range	Value (m)	Range	Value (m)
$IR_B(\text{FD})$	151	$IR_B(\text{FD})$	177
$IR_B(\text{HD})$	142	$IR_B(\text{HD})$	160
CSR_A	153	CSR_A	143
CSR_{AB}	251	CSR_{AB}	249

We have the same results for TR_C , $IR_C(\text{FD})$, $IR_C(\text{HD})$, CSR_D and CSR_{CD} .

6.3 Simulation Results and Analysis

When $D_{AB}/D_{CD}=80$, CSR_A/CSR_D can cover $IR_B(\text{HD})/IR_C(\text{HD})$. However, when $D_{AB}/D_{CD}=90$, CSR_A/CSR_D cannot cover $IR_B(\text{HD})/IR_C(\text{HD})$. Therefore, after B/C sends the DataB→A /DataC→D frame, according to our MAC protocol, in the former case, B/C only needs to receive the remainder of the data frame in the HD mode; but in the latter case, B/C should send a certain number of the ADD frames. Initially, we require that A first initiates a request to B, and the FD communication is first set up between the two nodes. We compare the system throughput for our MAC protocol and those of the typical FD MAC protocol in [11] and the HD DCF protocol.

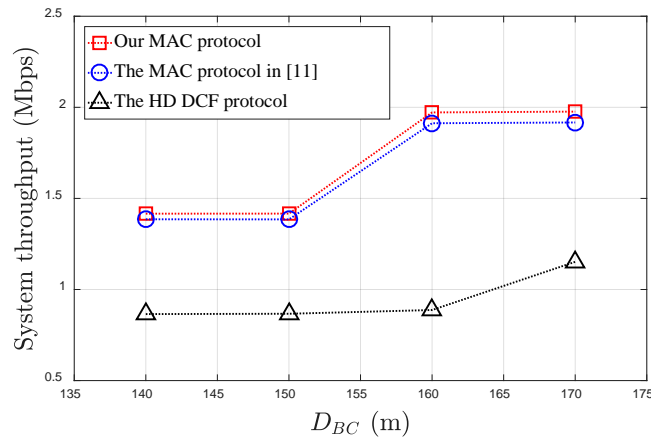


Fig. 15. The system throughputs for our MAC protocol, the MAC protocol in [11], and the HD DCF protocol with $D_{AB}/D_{CD}=80$.

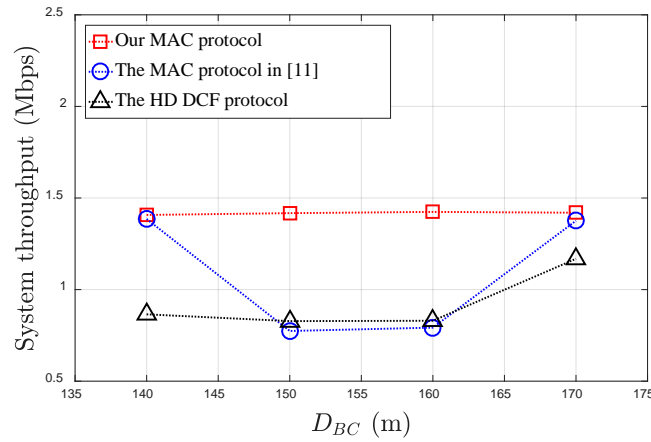


Fig. 16. The system throughputs for our MAC protocol, the MAC protocol in [11], and the HD DCF protocol with $D_{AB}/D_{CD}=90$.

As shown in Fig. 15 and Fig. 16, compared with the MAC protocol in [11] and the HD DCF protocol, our protocol can improve the system throughput. In the following discussion, we give the detailed analyses of the three protocols.

1). Detailed analyses for the three protocols with $D_{AB}/D_{CD}=80$ and varied D_{BC} .

The throughputs of each node for the three protocols with $D_{AB}/D_{CD}=80$ and varied D_{BC} are shown in Table 3.

Table 3. The throughputs of each node for the three protocols with $D_{AB}/D_{CD}=80$.

$D_{AB}/D_{CD}=80$	Protocol	A	B	C	D	Throughput
		(Packets number)				(Mbps)
(a). $D_{BC}=140$	Our MAC protocol	3415	3415	3666	3666	1.4162
	The MAC protocol in [11]	3493	3493	3434	3434	1.3854
	The HD DCF protocol	1845	2425	2597	2015	0.865
(b). $D_{BC}=150$	Our MAC protocol	3464	3463	3619	3619	1.41652
	The MAC protocol in [11]	3570	3570	3354	3354	1.3848
	The HD DCF protocol	2048	2547	2445	1847	0.8668
(c). $D_{BC}=160$	Our MAC protocol	4930	4930	4930	4930	1.972
	The MAC protocol in [11]	4781	4781	4782	4782	1.9126
	The HD DCF protocol	452	4894	4815	470	0.8874
(d). $D_{BC}=170$	Our MAC protocol	4941	4941	4941	4941	1.9764
	The MAC in protocol [11]	4792	4792	4792	4792	1.9168
	The HD DCF protocol	1568	4860	4797	1593	1.1519

When $D_{BC}=140$, $C \in IR_B(\text{HD})/B \in IR_C(\text{HD})$, but when $D_{BC}=150$, neither of them holds. However, $C \in CSR_A/B \in CSR_D$ always holds. As long as there exists the transmitted signal from A/D, C/B will not contend for the channel. The throughputs for the three protocols do not change much in the two cases. First, in our proposed protocol, on the one hand, after the DataB→A/DataC→D frame is sent, CSR_{AB}/CSR_{CD} will reduce to CSR_A/CSR_D , and D/A will start to send the request to C/B. However, C/B can still sense the transmitted signal of the

DataA→B/DataD→C frame and does not reply to the request. If D/A waits for a timeout, then it increases the size of contention window and reselect the back-off count. Moreover, if the number of the timeouts increase, then the probability that D/A gets a larger value of the back-off period will increase. On the other hand, A/D does not start to send the AckA→B/AckD→C frame until B/C has completed sending the AckB→A/AckC→D frame. Besides, C/B can sense the transmitted signal of the AckA→B/AckD→C frame. After the signal disappears, C/B needs to defer the EIFS time before contending for the channel. Therefore, although the two FD pairs work “alternately”, once an FD pair access the channel, the probability of them accessing the channel again is larger than that of the other FD pair. Thus, the numbers of data frames sent by the two pairs are inconsistent. Second, in the MAC protocol in [11], in order to ensure that B/C can receive the DataA→B/DataD→C frame successfully, it sets the virtual carrier-sensing time for the nodes located in the TR_B/TR_C . However, note that $C \notin IR_B(HD)/B \notin IR_C(HD)$, in fact, C/B does not need to set this time. The three-handshake mechanism in [11] reduces the channel utilization, so the system throughput produced by that protocol is slightly lower than our protocol. Third, in the HD DCF protocol, during the transmission of the DataA→B/DataD→C frame, C/B cannot reply the request from D/A. Similar to the above discussion, D/A may get a large value of the back-off period. So the probability of C/B accessing the channel is larger than that of D/A. Furthermore, when C/B transmits the signal, the other FD pair can sense it and do not contend for the channel. There is always only one HD communication in the system. Therefore, the throughput produced by this protocol is lower than those of the two protocols above.

When $D_{BC}=160$ or 170 , $C \notin IR_B(HD)/B \notin IR_C(HD)$ and $C \notin CSR_A/B \notin CSR_D$. First, in our protocol, after B/C sends the DataB→A/DataC→D frame, C/A and D/B can set up another FD communication, which will execute simultaneously with the remaining transmission of the DataA→B/DataD→C frame. At this time, our protocol produces its maximum throughput. Second, in the protocol in [11], when $D_{BC}=160$, $C \in TR_B/B \in TR_C$. In theory, the control frame sent by B/C will prevent C/B from accessing the channel even though B/C sends over. However, in our simulation, this exposed terminal problem is not obvious. Because each node has a saturated queue of data frames to send, for C, the request from D is likely to interfere with the reception of the control frame sent by B. If C fails to receive the control frame, its virtual carrier-sensing time cannot be properly set. C will contend for the channel after B sending the DataB→A frame. During the control frames interaction of C and D, B receives the remainder of the DataA→B frame; it will not receive the control frame sent by C. After the DataC→D frame is sent, A and B can also set up another FD commutation. Note that when $D_{BC}=170$, $C \notin TR_B/B \notin TR_C$, C and B cannot receive the control frame from each other. The working process of the protocol in such case is similar with that in $D_{BC}=160$ case. In the two cases, the system throughput for the MAC protocol in [11] is similar with that of our protocol. Third, in the HD DCF protocol, when $D_{BC}=160$, the probabilities of B and C accessing the channel are even larger than those in $D_{BC}=140$ and 150 cases. At this time, $D \notin CSR_B$ and $C \in TR_B/A \notin CSR_C$ and $B \in TR_C$. For one thing, D/A cannot sense the transmitted signals from B/C. For another, C/B may be set the virtual carrier-sensing time by B/C. During the transmission of the DataB→A/DataC→D frame, D/A contends for the channel ineffectively, which reduces its probability for accessing the channel. When $D_{BC}=170$, D/A will get more opportunities to access the channel because $D_{BC} > TR_B/TR_C$. The throughput can be improved.

2). Detailed analyses for the three protocols with $D_{AB}/D_{CD}=90$ and varied D_{BC} .

The throughputs of each node for the three protocols with $D_{AB}/D_{CD}=90$ and varied D_{BC} are shown in Table 4.

Table 4. The throughputs of each node for the three protocols with $D_{AB}/D_{CD}=90$.

$D_{AB}/D_{CD}=90$	Protocol	A	B	C	D	Throughput
		(Packets number)				(Mbps)
(a). $D_{BC}=140$	Our MAC protocol	3403	3403	3635	3635	1.4076
	The MAC protocol in [11]	3429	3429	3498	3498	1.3854
	The HD DCF protocol	1845	2425	2597	2015	0.865
(b). $D_{BC}=150$	Our MAC protocol	3532	3532	3555	3555	1.4174
	The MAC protocol in [11]	1876	1877	1995	1994	0.77416
	The HD DCF protocol	220	4882	4745	262	0.828
(c). $D_{BC}=160$	Our MAC protocol	3587	3587	3534	3534	1.4242
	The MAC protocol in [11]	1856	1861	2107	2103	0.79252
	The HD DCF protocol	234	4876	4774	246	0.8304
(d). $D_{BC}=170$	Our MAC protocol	3397	3397	3702	3702	1.41972
	The MAC protocol in [11]	2735	4914	4913	2180	1.37596
	The HD DCF protocol	1671	4781	4835	1654	1.1683

When $D_{BC}=140$, the system throughput for our protocol is slightly lower than that in $D_{AB}/D_{CD}=80$ and $D_{BC}=140$ case. In such case, after B/C sends the DataB→A/DataC→D frame, the continuous ADD frames sent by it can freeze the back-off count of D/A, so that D/A will not send the ineffective request and its back-off count will not increase. Thus, the probability of D/A accessing the channel becomes larger. However, when the transmit requests of A and D overlap, during the B and C receiving the desired requests, they can sense the other signal, according to our protocol, neither B nor C will reply. Therefore, the overlapping time is wasted. When $D_{BC}=150, 160$ and 170 , in such case, at least one of B and C will reply the CTS-M frame, so the system throughput is improved as compared with that in $D_{BC}=140$ case.

For the MAC protocol in [11] and the HD DCF protocol, their working processes in such case are consistent with those in $D_{AB}/D_{CD}=80$ and $D_{BC}=140$ case.

When $D_{BC}=150$ and 160 , $C \in IR_B(\text{HD})/B \in IR_C(\text{HD})$, but $C \notin CSR_A/B \notin CSR_D$. Although $C \in TR_B/B \in TR_C$, using the “Duration” field of the control frame to reserve the channel only has limited effectiveness. The system throughput for the MAC protocol in [11] even lower than that of the HD DCF protocol. We assume that A communicates with B in the FD mode. We also assume that the control frame sent from B to C has been interfered. After B sends the DataB→A frame, C and D will set up the other FD communication. But the transmitted signal of C will interfere with the remaining reception of the DataA→B frame. In addition, although A can receive the DataB→A frame correctly, the reception of the AckA→B frame will be interfered. Thus, the FD communication between A and B do not produce any effective throughput. Similarly, after C sends the DataC→D frame, the following FD communication between A and B will interfere with the remaining receptions of the DataD→C frame and the AckD→C frame. As the number of the timeouts increases, the back-off count of each node will increase. The protocol will not produce effective throughput again until C/B can keep silence during the remaining reception of DataA→B/DataD→C frame. In the HD DCF protocol, once C/B does not correctly receive the control frame sent from B/C, the subsequent transmitted signal of C/B will interfere with the reception of the DataA→B/DataD→C frame. Therefore, the system throughput for the protocol in $D_{AB}/D_{CD}=90$ and $D_{BC}=150$ or 160 case is lower than that in D_{AB}

$/D_{CD}=90$ and $D_{BC}=160$ case.

When $D_{BC}=170$, $C \notin TR_B/B \notin TR_C$. In addition, although $C \notin IR_B(\text{HD})/B \notin IR_C(\text{HD})$, we have $C \in IR_B(\text{FD})/B \in IR_C(\text{FD})$. In the MAC protocol in [11], C/B cannot receive the control frame from B/C correctly. After B/C sends the DataB→A/DataC→D frame, C/B and D/A will set up the other FD communication. But the reception of the DataD→C/DataA→B frame will definitely be interfered with the AckB→A/AckC→D frame. In other words, if C/B starts to communicate with D/A in the FD mode before B/C sending the AckB→A/AckC→D frame, C/B cannot receive the DataD→C/DataA→B frame correctly. The HD DCF protocol has the similar performance with that in $D_{AB}/D_{CD}=80$ and $D_{BC}=170$ case.

7. Conclusions

In FD networks, we proposed a MAC protocol to alleviate hidden terminal problems. We presented the FD interference model and discussed the interference risks in FD networks. Then, we summarized the existing methods and their effective conditions for collision avoidance in HD networks. We extended the methods to FD networks and developed a feasible FD MAC protocol. The simulation results validated our protocol.

The proposed MAC protocol in this paper is for the bidirectional mode of the FD nodes. Whereas the other transmission mode of the FD nodes is wormhole-relaying. In such mode, each node may act as one of the three roles (sender, relay or receiver). The relevant ranges of nodes are related to their roles. Therefore, the follow-up work needs to consider how to identify or even designate the role of each node first and then coordinate sender and relay to access the channel simultaneously.

References

- [1] A. Sabharwal, P. Schniter, D. Guo, et al., "In-band full-duplex wireless: Challenges and opportunities," *IEEE Journal on Selected Areas in Communications*, vol. 32, no. 9, pp. 1637–1652, 2014. [Article \(CrossRef Link\)](#).
- [2] T. Maksymyuk, M. Kyryk, M. Jo, "Comprehensive Spectrum Management for Heterogeneous Networks in LTE-U," *IEEE Wireless Communications*, Vol.23, No.6, pp.8-15, 2016. [Article \(CrossRef Link\)](#).
- [3] X. Xie and X. Zhang, "Does full-duplex double the capacity of wireless networks?," in *Proc. of the 33rd Annual IEEE International Conference on Computer Communications (INFOCOM)*, Toronto, Canada, pp.253–261, Apr. 2014. [Article \(CrossRef Link\)](#).
- [4] D. Kim, H. Lee, D. Hong, "A survey of in-band full-duplex transmission: From the perspective of phy and mac layers," *IEEE Communications Surveys and Tutorials*, vol. 17, no. 4, pp. 2017–2046, Apr. 2015. [Article \(CrossRef Link\)](#).
- [5] K. Xu, M. Gerla, S. Bae, et al., "How effective is the ieee 802.11 rts/cts handshake in ad hoc networks," in *Proc. of IEEE global communications conference (GLOBECOM)*, Taipei, Taiwan, pp. 72–76, Nov. 2002. [Article \(CrossRef Link\)](#).
- [6] K. Shih, Y. Chen, "Capc: a collision avoidance power control mac protocol for wireless ad hoc networks," *IEEE Wireless Communications Letters*, vol. 9, no. 9, pp. 859–861, 2005. [Article \(CrossRef Link\)](#).
- [7] Y. Zhou, S. M. Nettles, "Balancing the hidden and exposed node problems with power control in csma/ca-based wireless networks," in *Proc. of IEEE Wireless Communications and Networking Conference (WCNC)*, New Orleans, LA, USA, pp. 683–688, Mar. 2005. [Article \(CrossRef Link\)](#).
- [8] The Omnet++ simulator. <https://www.omnetpp.org>

- [9] M. Jain, J. I. Choi, T. Kim, et al., "Practical, real-time, full duplex wireless," in *Proc. of the 17th ACM Annual International Conference on Mobile Computing and Networking (MobiCom)*, pp. 301–312, 2011. [Article \(CrossRef Link\)](#).
- [10] Y. Zhang, L. Lazos, K. Chen, et al., "FD-MMAC: Combating multi-channel hidden and exposed terminals using a single transceiver," in *Proc. of the 33rd Annual IEEE International Conference on Computer Communications (INFOCOM)*, Toronto, Canada, pp. 2742–2750, Apr. 2014. [Article \(CrossRef Link\)](#).
- [11] X. Zhang, W. Cheng, H. Zhang, "Full-duplex transmission in phy and mac layers for 5G mobile wireless networks," *IEEE Wireless Communications*, vol. 22, no. 5, pp. 112–121, 2015. [Article \(CrossRef Link\)](#).
- [12] R. Liao, B. Bellalta, M. Oliver, "Modelling and enhancing full-duplex mac for single-hop 802.11 wireless networks," *IEEE Wireless Communications Letters*, vol. 4, no. 4, pp. 349–352, 2015. [Article \(CrossRef Link\)](#).
- [13] D. Marlali, O. Gurbuz, "S-CW FD: A MAC Protocol for Full-Duplex in Wireless Local Area Networks," in *Proc. of IEEE Wireless Communications and Networking Conference (WCNC)*, Doha, Qatar, pp. 1–6, Apr. 2016. [Article \(CrossRef Link\)](#).
- [14] A. Tang, X. Wang, "A-Duplex: Medium Access Control for Efficient Coexistence Between Full-Duplex and Half-Duplex Communications," *IEEE Transactions on Wireless Communications*, vol. 14, no. 10, pp. 5871–5885, 2015. [Article \(CrossRef Link\)](#).
- [15] W. Choi, H. Lim, A. Sabharwal, "Power-controlled medium access control protocol for full-duplex wifi networks," *IEEE Transactions on Wireless Communications*, vol. 14, no. 7, pp. 3601–3613, 2015. [Article \(CrossRef Link\)](#).
- [16] O. M. Alkadri, A. Aijaz, A. Nallanathan, "An energy-efficient full-duplex mac protocol for distributed wireless networks," *IEEE Wireless Communications Letters*, vol. 5, no. 1, pp. 44–47, 2016. [Article \(CrossRef Link\)](#).
- [17] Y. Song, W. Qi, W. Cheng, "Energy efficient MAC protocol for wireless full-duplex networks," *China Communications*, vol. 15, no. 1, pp. 35–44, 2018. [Article \(CrossRef Link\)](#).
- [18] G. Bianchi, "Performance analysis of the IEEE 802.11 distributed coordination function", *IEEE Journal on Selected Areas in Communications*, vol. 18, no. 3, pp. 535–547, March 2000. [Article \(CrossRef Link\)](#).



SONG Yu (1983-), received the Ph. D. degree in Computer Science and Technology from PLA Army Engineering University, China, in 2018. Now he is a lecturer in Information and Communications College, National University of Defense Technology (NUDT), China. His research interests are primarily in the MAC protocol designs of wireless full-duplex network and cognitive wireless networks.

Email: ys_yusong@163.com.



QI Wangdong (1968-), the corresponding author, received the Ph. D. degree from Institute of Communication Engineering, China, in 1992. Now he is a professor in National Mobile Communications Research Laboratory, Southeast University, China. His research interests include wireless sensor network node localization, anti-jamming navigation and positioning technology and network security technology, etc.

Email: wangdongqi@gmail.com.



CHENG Wenchi (1986-), received the B.S. degree and Ph.D. degree in Telecommunication Engineering from Xidian University, China, in 2008 and 2014, respectively. He joined Department of Telecommunication Engineering, Xidian University, in 2013, where he is an Associate Professor. His research interests focus on 5G wireless networks, wireless full-duplex transmission, statistical QoS provisioning, cognitive radio techniques, and energy efficient wireless networks.

Email: wccheng@xidian.edu.cn.